Low oxygen waters limited habitable space for early animals

Low oxygen waters limited habitable space for early animals

R Tostevin[1*], R A Wood[2], G A Shields[1], S W Poulton[3], R Guilbaud[4], F Bowyer[2], A M Penny[2], T He[1], A Curtis[2], K H Hoffman[5], M O Clarkson[2]

[1]*Department of Earth Sciences, University College London, Gower Street, London,* WC1E 6BT, UK

[2]*School of GeoSciences, The University of Edinburgh, James Hutton Road, Edinburgh EH9 3FE*

[3]*School of Earth and Environment, University of Leeds, Leeds, LS2 9JT, UK*

[4]*Department of Earth Sciences, University of Cambridge, Downing Street, Cambridge, CB2 3EQ, UK*

[5]*Geological Survey of Namibia, Private Bag 13297, Windhoek, Namibia*

*Correspondence to Rosalie Tostevin: Rosalie.tostevin@earth.ox.ac.uk. Current address: Department of Earth Sciences, University of Oxford, Oxford, OX1 3AN, UK

The oceans at the start of the Neoproterozoic Era (1000-541 million years ago, Ma) were dominantly anoxic, but may have become progressively oxygenated, coincident with the rise of animal life. However, the control that oxygen exerted on the development of early animal ecosystems remains unclear, as previous research has focussed only on the identification of fully anoxic or oxic conditions, rather than intermediate redox levels. Here, we report anomalous cerium enrichments preserved in carbonate rocks across bathymetric basin transects from nine localities of the Nama Group, Namibia (~550-541 Ma). In combination with Fe-based redox proxies, these data suggest that low oxygen conditions occurred in a narrow zone between well-oxygenated surface waters and fully anoxic deep waters. Although abundant in well-oxygenated environments, early skeletal animals did not occupy

oxygen impoverished regions of the shelf, demonstrating that oxygen availability (likely >10 μM) was a key requirement for the development of early animal-based ecosystems.

Geochemical proxies based on Fe-S-C and trace metal systematics have been widely used to reconstruct the progressive oxygenation of the oceans during the Neoproterozoic and Cambrian[1–7]. Accumulating evidence indicates that the deep oceans were dominantly anoxic and ferruginous (Fe-containing) throughout most of the Precambrian, with euxinic (sulphidic) mid-depth waters prevalent along continental margins from ~1.8 to 1.0 billion years ago (Ga)[1,6,8]. From ~1.0 to 0.58 Ga, however, euxinic mid-depth waters became less prevalent and ferruginous conditions expanded, with oxic conditions still largely restricted to surface waters[1,8,9]. The oxygenation of the deeper marine realm was both protracted and spatially heterogeneous, with some marine basins recording persistent deep-water oxygenation from ~580 Ma, whereas regional anoxia remained a feature of some deeper shelf environments into the Cambrian, ~520 Ma[4,5,7,10] and beyond.

The course of Neoproterozoic oxygenation, and cause and effect associations with the appearance of animals, remains controversial[4,11–13]. While modern soft-bodied sponge-grade animals may tolerate oxygen concentrations as low as 1.25-10 μM[15], new innovations in the late Ediacaran, such as motility[16], the rise of predation, and skeletonisation[17–19], are all hypothesised to have required higher levels of oxygen[20]. However, the oxygen demands of early animals are unconstrained, and observations

53 from modern biota cannot necessarily be applied to early animals of unknown
54 affinity. Furthermore, while soft-bodied and skeletal Ediacaran fauna dominantly
55 occur in sediments interpreted to have been deposited from oxic waters, fossil
56 occurrences have also been reported in sediments characterised by anoxic
57 geochemical signals[5,14]. In the latter case, this may be because some early complex
58 organisms were able to colonise habitats during fleeting periods of oxia (such short-
59 lived oxygenation is difficult to detect by geochemical proxies that tend to integrate
60 relatively long periods of time). In both of the above cases, however, there is
61 uncertainty as to whether early animal evolution occurred under fully oxygenated
62 conditions, or whether intermediate redox conditions were more prevalent, which
63 by extension suggests that the oxygen requirements of more complex organisms
64 were lower[3,15]. An in-depth understanding of these links is currently hampered,
65 however, by the inability of most redox proxies to distinguish between fully
66 oxygenated and intermediate redox states, including nitrogenous or manganous
67 conditions, which may overlap with low concentrations of oxygen[16,17]. Indeed, it is
68 possible that 'oxic' horizons identified through Fe and trace element geochemistry
69 may in fact have formed under low oxygen conditions (but not fully anoxic), at levels
70 insufficient to support diverse skeletal animal communities.
71
72 In oxic environments, Ce(III) is oxidised to insoluble Ce(IV) and preferentially
73 scavenged relative to the rest of the rare earth elements and yttrium, REY[18]. The
74 standard reduction potential of Ce(IV) (+1.61˚V) is closer to Mn(IV) (+1.23˚V) than
75 Fe(III) (+0.77˚V), and Ce oxidation is catalysed on the surface of Mn

(oxyhydr)oxides[19]. Therefore, the redox cycling of Ce in seawater is closely related to Mn(II)/Mn(IV) transformations, which occur at a higher redox potential than the Fe(II)/Fe(III) couple, and hence Mn cycling is more sensitive to intermediate redox conditions[18–21]. Ce anomalies (Ce_{SN}/Ce^*_{SN}) are calculated here based on relative enrichments or depletions in shale-normalised Ce ($[Ce]_{SN}$) compared to neighbouring non-redox sensitive REY:

$$Ce_{SN}/Ce^*_{SN} = \frac{[Ce]_{SN}}{([Pr]_{SN})^2/[Nd]_{SN}} \quad (1)$$

Due to the accumulation of Ce(IV) on the surface of Mn (oxyhydr)oxides, oxic seawater becomes Ce-depleted and exhibits a negative Ce anomaly (<0.9)[18] (see Methods and Supplementary Information for discussion of Ce/Ce* thresholds). These Mn (oxyhydr)oxides may be buried intact in sediments beneath oxic bottom waters, or may dissolve in the water column if they encounter low oxygen waters, releasing excess Ce. Therefore, waters beneath the Mn(IV)/Mn(II) redoxcline commonly exhibit a positive Ce anomaly (>1.3)[20–22]. Positive Ce anomalies have been recorded alongside Mn enrichments in some modern waters, including Lake Vanda, Antarctica (Ce_{SN}/Ce^*_{SN} up to 2.3, Fig 1)[20], in anoxic brines in the eastern Mediterranean (Ce_{SN}/Ce^*_{SN} up to 2.43, Fig 1)[22], and in the deep-marine Cariaco Basin (Ce_{SN}/Ce^*_{SN} up to 1.21)[21].

Water column REY, and associated Ce anomalies, are thought to be preserved in non-skeletal carbonate rocks without fractionation[23]. Carbonate-bound REY are relatively robust to diagenetic alteration[23] and dolomitisation[24], but any alteration

of the Ce anomaly can be identified using non-redox sensitive REY anomalies, such as the Y/Ho ratio, which would also be altered away from seawater patterns[25,26]. We use a sequential dissolution method that targets REY in the carbonate phase, preventing contributions from sedimentary (oxyhydr)oxides or clays[26], which would carry a non-seawater signature. The majority of samples are very pure calcites with low siliciclastic components, but where samples are partially dolomitised they have been treated differently during leaching[26]. The resulting REY data have been screened for traditional seawater features (Y/Ho ratios >67), and samples with evidence for diagenetic alteration or contributions from non-carbonate phases have been excluded from the presented Ce/Ce* data (see Methods and Supplementary Information).

We additionally utilise redox interpretations based on published Fe speciation data for these carbonate samples[5]. Fe-speciation distinguishes anoxic from oxic water column conditions through enrichments in highly reactive Fe (Fe_{HR}) relative to total Fe (Fe_T)[1,27]. Anoxic enrichments in Fe_{HR} occur due to the water column formation of either pyrite under euxinic conditions[27], or non-sulphidized Fe_{HR} minerals (such as Fe oxides or carbonates) under anoxic ferruginous conditions[1] (see Methods). Although originally calibrated for siliciclastics[1,27], enrichments in Fe_{HR}/Fe_T can also be identified in carbonates deposited under anoxic water column conditions[28]. These Fe_{HR} enrichments can far exceed Fe_{HR} contents expected under normal oxic deposition, where trace amounts (~0.1 wt%) of Fe may be incorporated into carbonates, or precipitate as Fe-Mn coatings[28]. However, while early dolomitisation

in shallow burial environments does not generally cause a significant increase in Fe_{HR}, late stage deep burial dolomitisation may significantly increase Fe_{HR}, but there is no petrographic evidence for deep burial dolomitisation in our samples[5,29]. Consistent with a recent calibration[28], we have limited the application of Fe-speciation to carbonate samples with >0.5wt% Fe_T, which buffers against the impact of non-depositional enrichments in Fe_{HR}[28]. In addition, however, we stress that all of our redox interpretations based on Fe speciation in carbonates are entirely consistent with data for interbedded siliciclastics[5].

Results

In the present study, we measured REY in 259 carbonate rocks of the Nama Group from nine sites across two basins. The succession was deposited ~550-541 Ma broadly coincident with the first appearance of skeletal animals[29–31], as well as trace fossil evidence for motility[32] and soft-bodied fossils belonging to the Ediacaran biota[33]. Our samples cover a range of palaeo-depths from shallow inner ramp to deeper outer ramp waters, in the Kanies, Omkyk and Hoogland Members of the Kuibis Subgroup, and the Spitzkopf and Feldschuhorn Members of the upper Schwarzrand Subgroup[5,29] (Fig 2; see Supplementary Information for full details of the geological setting). We focus on the first known skeletal animals, *Cloudina*, a globally distributed eumetazoan of possible cnidarian affinity[30,34,35]; *Namacalathus*, interpreted as a stem group eumetaozan[36] or triploblast lophophorate[37] and reported from multiple localities; and *Namapoikia*, an encrusting possible cnidarian or poriferan known only from the Nama Group[31].

144

145 In the Nama Group, the majority of REY distribution patterns are smooth and show a
146 flat or light REY-depleted shape on shale-normalised plots, positive La anomalies,
147 low total REE concentrations, and superchondritic Y/Ho ratios (>67), all of which
148 indicate preservation and extraction of original seawater signals (see
149 Supplementary Information for a description of all data). Four samples exhibit
150 negative Ce anomalies (<0.9) (Fig 2), consistent with an oxic water column
151 interpretation obtained for these samples from Fe-speciation[5]. Ce anomalies are, as
152 expected, absent from the persistently anoxic and ferruginous deepest water
153 setting[5] (Fig 2). Significant positive Ce anomalies (1.30 - 2.15) are, however,
154 prevalent in inner ramp sections in both sub-basins (64 samples). In six cases
155 positive Ce anomalies are associated with anoxic ferruginous signals, and in one
156 case, a positive Ce anomaly is associated with a sample that gives a robust oxic
157 Fe_{HR}/Fe_T signal. However, for the majority of samples (~90%), Fe_T was <0.5 wt%,
158 preventing a robust evaluation of water column redox conditions from Fe speciation
159 alone. In these cases, samples have elevated Mn/Fe ratios (median = 0.39), when
160 compared to samples with no positive Ce anomalies (median = 0.14) and anoxic
161 ferruginous samples (median = 0.10), which provides an independent constraint on
162 water column redox conditions, as discussed below (Fig 3).
163

164 The regionally widespread positive Ce anomalies across the Zaris and Witputs
165 Basins of the Nama Group imply a surplus of Ce sustained by a rain-down of Mn
166 (oxyhydr)oxides from shallow oxygenated surface waters, and this is supported by

167 the elevated Mn/Fe ratios of these samples (Fig 3). Redox cycling of Mn
168 (oxyhydr)oxides across the Mn(IV/II) redoxcline would leave ambient waters
169 locally enriched in the Ce released during Mn(IV) reduction (Fig 1). We therefore
170 interpret positive Ce anomalies (>1.3) to indicate intermediate manganous
171 conditions. Where there is an absence of both positive Ce anomalies and any
172 indication of enrichment in Fe (i.e., Fe_{HR}/Fe_T<0.22 or Fe_T <0.5 wt%), we suggest that
173 bottom waters were likely well-oxygenated (which is consistent with Fe_{HR}/Fe_T
174 signals in interbedded siliciclastics[5]), thus preventing the onset of both Fe and Mn
175 reduction. Where data are equivocal (e.g., Fe_{HR}/Fe_T between 0.22-0.38 and no Ce
176 anomaly), we are unable to interpret redox conditions.
177
178 The outer ramp was persistently anoxic and ferruginous (Brak section) and animals
179 are absent from these settings[5] (Fig 4). The deep inner-ramp sections show periods
180 of anoxic ferruginous, manganous and well-oxygenated conditions (Zebra River and
181 Omkyk sections). In these settings, animals are notably absent from ferruginous and
182 manganous waters, whereas well-oxygenated waters support abundant skeletal
183 animals, up to 35 mm in diameter, and adjacent localities show trace fossil evidence
184 for motility[32]. The shallowest inner ramp sections show high-frequency temporal
185 fluctuations between anoxic ferruginous, manganous and well-oxygenated
186 conditions (Zwartmodder, Arasab and Grens sections), as might be expected due to
187 fluctuations in the depth of the chemocline (Fig 4). At Zwartmodder, skeletal
188 animals are present in thin beds[5], but there is only one skeletal horizon at Grens,
189 and no animal fossils at Arasab.

In contrast to these ecologies, the Driedoornvlagte pinnacle reef grew within a transgressive systems tract in a mid-ramp position, which was persistently well-oxygenated and hosts some very large skeletal animals[5,31] (up to 1 m) and complex reef-building ecologies[30]. In the younger Schwarzrand Subgroup, which extends close to the Ediacaran-Cambrian Boundary (~547-541 Ma), there is evidence for persistent well-oxygenated conditions[5] and mid-ramp Pinnacle Reefs host mixed communities of large and small skeletal animals. At Swartpunt, abundant burrows and soft-bodied biota occur in siliciclastic horizons, where Fe speciation indicates oxic conditions[5], while small *in-situ* skeletal animals are found in carbonate rocks throughout the succession[5].

Discussion

Our geochemical and palaeontological data demonstrate a striking relationship between the precise redox condition of the water column and the presence and abundance of evidence for animal life. Constraints from the modern open ocean suggest that dissolved Mn(II), and therefore Ce(III), can start to build up in low concentrations in oxic waters with dissolved O_2 <100 μM[17]. However, manganous conditions, whereby Mn becomes the dominant redox buffer, are achieved at lower oxygen concentrations. Reduced Mn can remain stable in the presence of up to 10 μM O_2[16,38], although Mn oxidation has been reported locally at lower O_2 concentrations where oxidation is catalysed by enzymatic processes[39]. Thus, active Mn cycling can occur in anoxic waters, but is commonly documented in partially oxic

213 waters with at least 10 μM O_2 (and up to 100 μM O_2; Fig 1)[16,38,40,41], which represents
214 significant oxygen depletion in comparison to modern fully oxygenated surface
215 waters (~250 μM O_2). The reduction potential for Ce is higher than that for Mn, and
216 so the 10 μM O_2 constraint for manganous waters may represent a lower limit on Ce
217 cycling, as sufficient O_2 to oxidise both Ce and Mn is required for the formation of Ce
218 anomalies.
219
220 Our multi-proxy approach allows us to distinguish between fully anoxic and
221 intermediate waters, which contained low but significant amounts of oxygen. Where
222 Fe-speciation in Ce enriched samples gives a robust anoxic signal (Fe_{HR}/Fe_T >0.38),
223 Mn reduction may have persisted, but conditions must have been fully anoxic.
224 However, the majority of samples interpreted to be manganous have insufficient Fe_T
225 for Fe-speciation (with 85% of these falling below 0.25 wt% Fe_T, and 35% falling
226 below 0.1 wt% Fe_T). Even very low oxygen concentrations (nM) are sufficient to
227 prevent highly reactive Fe enrichments, and so the low Fe_T in shallower
228 environments across the Nama Group may be indicative of oxic conditions[42], and
229 this is supported by persistent oxic Fe_{HR}/Fe_T ratios obtained from interbedded
230 siliciclastics in some sections[5]. We therefore suggest that the manganous zone
231 occurred between well-oxygenated surface waters and deeper anoxic, ferruginous
232 waters, commonly overlapping with low but significant concentrations of oxygen (at
233 least ~10 μM) (Fig 1).
234

Oxygen exerts an important control on ecosystem structure in modern environments, whereby low oxygen environments are inhabited by smaller animals often lacking skeletons and forming low diversity communities with simple food webs[43]. In general, skeletons are absent from modern oxygen minimum zones when O_2 drops below 13 μM, and large animals are often absent below 45 μM [refs [44,45]]. However, the importance of oxygen in supporting early animal ecosystems as they became increasingly complex in form, metabolic demand, and behaviour through the Ediacaran Period is currently unresolved[2,3,5,11–13]. In the Nama Group the majority of small skeletal animals (>75%), and all evidence for large skeletal animals, motility, soft-bodied biota and complex ecologies[30], are found in sediments deposited from well-oxygenated waters (Fig 4). The identification of low-oxygen, manganous water column conditions thus provides a compelling explanation for the general absence of biota in these settings, and implies that poorly oxygenated conditions were insufficient to meet the relatively high oxygen requirements of these early skeletal animals[5,30,32,33]. If we take an upper O_2 limit for Mn and Ce reduction of 10 μM O_2, this suggests that Mn-enriched waters could theoretically support small, soft-bodied animals, such as sponges[15]. In contrast, the absence of skeletal animals in Mn-enriched waters is consistent with the high energetic cost of skeletonisation. Possible biomarkers for sponge animals appear in the fossil record at >635 Ma [Ref 46], but it is possible that the availability of well-oxygenated habitats was necessary to support the later appearance of skeletonisation, at ~550 Ma. However, it is also unlikely that reaching an oxygenation threshold alone is sufficient to explain the appearance of skeletons[47], and many have argued that the

trigger for the rise of skeletonisation may have been ecological, such as the rise of predation[36,48].

Our approach highlights that intermediate redox conditions were probably widespread in the Ediacaran ocean, but have not previously been appreciated due to the inability of most commonly used proxies to identify such conditions. Our data suggest that low oxygen water column conditions were insufficient to support early skeletal and reef-building animals, and so the extent of suitable habitat space may have been less than previously identified. The widespread radiation of skeletal animals during the subsequent Cambrian explosion may have been facilitated by a global rise in the extent of habitable, oxygenated seafloor[7], alongside other genetic and ecological factors. Our data therefore yield new insight into the debate on the role of oxygen in early animal evolution, suggesting that well-oxygenated waters were necessary to support the appearance of the skeletal animals and complex ecologies that are typical of the terminal Neoproterozoic.

1. Poulton, S. W. & Canfield, D. E. Ferruginous Conditions: A Dominant Feature of the Ocean through Earth's History. *ELEMENTS* **7,** 107–112 (2011).
2. Johnston, D. T. *et al.* Late Ediacaran redox stability and metazoan evolution. *Earth and Planetary Science Letters* **335,** 25–35 (2012).
3. Planavsky, N. J. *et al.* Low Mid-Proterozoic atmospheric oxygen levels and the delayed rise of animals. *Science* **346,** 635–638 (2014).
4. Canfield, D. E., Poulton, S. W. & Narbonne, G. M. Late-Neoproterozoic Deep-Ocean Oxygenation and the Rise of Animal Life. *Science* **315,** 92 –95 (2007).
5. Wood, R. A. *et al.* Dynamic redox conditions control late Ediacaran ecosystems in the Nama Group, Namibia. *Precambrian Research* **261,** 252–271 (2015).
6. Scott, C. *et al.* Tracing the stepwise oxygenation of the Proterozoic ocean. *Nature* **452,** 456–459 (2008).
7. Chen, X. *et al.* Rise to modern levels of ocean oxygenation coincided with the Cambrian radiation of animals. *Nat Commun* **6,** (2015).
8. Poulton, S. W., Fralick, P. W. & Canfield, D. E. Spatial variability in oceanic redox structure 1.8 billion years ago. *Nature Geoscience* **3,** 486–490 (2010).
9. Guilbaud, R., Poulton, S. W., Butterfield, N. J., Zhu, M. & Shields-Zhou, G. A. A global transition to ferruginous conditions in the early Neoproterozoic oceans. *Nature Geosci* **8,** 466–470 (2015).
10. Sperling, E. A. *et al.* Statistical analysis of iron geochemical data suggests limited late Proterozoic oxygenation. *Nature* **523,** 451–454 (2015).

11. Nursall, J. Oxygen as a prerequisite to the origin of the Metazoa. *Nature* **183,** 1170–1172 (1959).
12. Lenton, T. M., Boyle, R. A., Poulton, S. W., Shields-Zhou, G. A. & Butterfield, N. J. Co-evolution of eukaryotes and ocean oxygenation in the Neoproterozoic era. *Nature Geoscience* (2014).
13. Butterfield, N. J. Oxygen, animals and oceanic ventilation: an alternative view. *Geobiology* **7,** 1–7 (2009).
14. Sperling, E. A. *et al.* Oxygen, facies, and secular controls on the appearance of Cryogenian and Ediacaran body and trace fossils in the Mackenzie Mountains of northwestern Canada. *Geological Society of America Bulletin* B31329.1 (2015).
15. Mills, D. B. *et al.* Oxygen requirements of the earliest animals. *Proceedings of the National Academy of Sciences* **111,** 4168–4172 (2014).
16. Johnson, K. S. *et al.* Manganese Flux from Continental Margin Sediments in a Transect Through the Oxygen Minimum. *Science* **257,** 1242–1245 (1992).
17. Klinkhammer, G. P. & Bender, M. L. The distribution of manganese in the Pacific Ocean. *Earth and Planetary Science Letters* **46,** 361–384 (1980).
18. Sholkovitz, E. R., Landing, W. M. & Lewis, B. L. Ocean particle chemistry: The fractionation of rare earth elements between suspended particles and seawater. *Geochimica et Cosmochimica Acta* **58,** 1567–1579 (1994).
19. Ohta, A. & Kawabe, I. REE (III) adsorption onto Mn dioxide (MnO_2) and Fe oxyhydroxide: Ce (III) oxidation by MnO_2. *Geochimica et Cosmochimica Acta* **65,** 695–703 (2001).

20. De Carlo, E. H. & Green, W. J. Rare earth elements in the water column of Lake Vanda, McMurdo Dry Valleys, Antarctica. *Geochimica et Cosmochimica Acta* **66,** 1323–1333 (2002).
21. de Baar, H. J. ., German, C. R., Elderfield, H. & van Gaans, P. Rare earth element distributions in anoxic waters of the Cariaco Trench. *Geochimica et Cosmochimica Acta* **52,** 1203–1219 (1988).
22. Bau, M., Möller, P. & Dulski, P. Yttrium and lanthanides in eastern Mediterranean seawater and their fractionation during redox-cycling. *Marine Chemistry* **56,** 123–131 (1997).
23. Webb, G. E. & Kamber, B. S. Rare earth elements in Holocene reefal microbialites: a new shallow seawater proxy. *Geochimica et Cosmochimica Acta* **64,** 1557–1565 (2000).
24. Banner, J. L., Hanson, G. N. & Meyers, W. J. Rare Earth Element and Nd Isotopic Variations in Regionally Extensive Dolomites From the Burlington-Keokuk Formation (Mississippian): Implications for Ree Mobility During Carbonate Diagenesis. *Journal of Sedimentary Research* **58,** (1988).
25. Tostevin, R. *et al.* Effective use of Ce anomalies as a redox proxy in carbonate dominated marine settings. (accepted). 
26. Himmler, T., Bach, W., Bohrmann, G. & Peckmann, J. Rare earth elements in authigenic methane-seep carbonates as tracers for fluid composition during early diagenesis. *Chemical Geology* **277,** 126–136 (2010).
27. Raiswell, R. & Canfield, D. E. Sources of iron for pyrite formation in marine sediments. *American Journal of Science* **298,** 219–245 (1998).

28. Clarkson, M. O., Poulton, S. W., Guilbaud, R. & Wood, R. A. Assessing the utility of Fe/Al and Fe-speciation to record water column redox conditions in carbonate-rich sediments. *Chemical Geology* **382**, 111-122 (2014).
29. Grotzinger, J. P., Watters, W. A. & Knoll, A. H. Calcified metazoans in thrombolite-stromatolite reefs of the terminal Proterozoic Nama Group, Namibia. *Paleobiology* **26,** 334 –359 (2000).
30. Penny, A. *et al.* Ediacaran metazoan reefs from the Nama Group, Namibia. *Science* **344,** 1504–1506 (2014).
31. Wood, R. A., Grotzinger, J. P. & Dickson, J. A. D. Proterozoic Modular Biomineralized Metazoan from the Nama Group, Namibia. *Science* **296,** 2383 – 2386 (2002).
32. Macdonald, F. A., Pruss, S. B. & Strauss, J. V. Trace fossils with spreiten from the late Ediacaran Nama Group,Namibia: complex feeding patterns five million years before the Precambrian–Cambrian boundary. *Journal of Paleontology* **88,** 299–308 (2014).
33. Hall, M. *et al.* Stratigraphy, palaeontology and geochemistry of the late Neoproterozoic Aar Member, southwest Namibia: Reflecting environmental controls on Ediacara fossil preservation during the terminal Proterozoic in African Gondwana. *Precambrian Research* **238,** 214–232 (2013).
34. Morris, S. C., Mattes, B. & Chen, M. The early skeletal organism Cloudina: new occurrences from Oman and possibly China. *American Journal of Science* 245–260 (1990).

35. Warren, L. V. *et al.* Corumbella and in situ Cloudina in association with thrombolites in the Ediacaran Itapucumi Group, Paraguay. *Terra Nova* **23,** 382–389 (2011).
36. Wood, R., A. Paleoecology of the earliest skeletal metazoan communities: Implications for early biomineralization. *Earth-Science Reviews* **106,** 184–190 (2011).
37. Zhuravlev, A. Y., Wood, R. A. & Penny, A. M. Ediacaran skeletal metazoan interpreted as a lophophorate. *Proc. R. Soc. B* **282,** 20151860 (2015).
38. German, C. R. & Elderfield, H. Rare earth elements in the NW Indian Ocean. *Geochimica et Cosmochimica Acta* **54,** 1929–1940 (1990).
39. Clement, B. G., Luther, G. W., III & Tebo, B. M. Rapid, oxygen-dependent microbial Mn(II) oxidation kinetics at sub-micromolar oxygen concentrations in the Black Sea suboxic zone. *Geochimica et Cosmochimica Acta* **73,** 1878–1889 (2009).
40. Saager, P. M., De Baar, H. J. W. & Burkill, P. H. Manganese and iron in Indian Ocean waters. *Geochimica et Cosmochimica Acta* **53,** 2259–2267 (1989).
41. Trefry, J. H., Presley, B. J., Keeney-Kennicutt, W. L. & Trocine, R. P. Distribution and chemistry of manganese, iron, and suspended particulates in Orca Basin. *Geo-Marine Letters* **4,** 125–130 (1984).
42. Raiswell, R. & Anderson, T. F. Reactive iron enrichment in sediments deposited beneath euxinic bottom waters: constraints on supply by shelf recycling. *Geological Society, London, Special Publications* **248,** 179–194 (2005).

383 43. Gibson, R. & Atkinson, R. Oxygen minimum zone benthos: adaptation and
384 community response to hypoxia. *Oceanography and Marine Biology: An Annual*
385 *Review* **41,** 1–45 (2003).
386 44. Levin, L. A., Gage, J. D., Martin, C. & Lamont, P. A. Macrobenthic community
387 structure within and beneath the oxygen minimum zone, NW Arabian Sea. *Deep*
388 *Sea Research* **47,** 189–226 (2000).
389 45. Savrda, C. E. & Bottjer, D. J. Oxygen-related biofacies in marine strata: an
390 overview and update. *Geological Society, London, Special Publications* **58,** 201–
391 219 (1991).
392 46. Love, G. D. *et al.* Fossil steroids record the appearance of Demospongiae during
393 the Cryogenian period. *Nature* **457,** 718–721 (2009).
394 47. Zhang, S. *et al.* Sufficient oxygen for animal respiration 1,400 million years ago.
395 *PNAS* **113,** 1731–1736 (2016).
396 48. Knoll, A. H. Biomineralization and Evolutionary History. *Reviews in Mineralogy*
397 *and Geochemistry* **54,** 329–356 (2003).
398 49. Turekian, K. K. & Wedepohl, K. H. Distribution of the Elements in Some Major
399 Units of the Earth's Crust. *Geological Society of America Bulletin* **72,** 175–192
400 (1961).
401 50. Grotzinger, J. & Miller, R. *The Nama Group*. **2,** (Geological Society of Namibia,
402 2008).
403 51. Bau, M. & Dulski, P. Distribution of yttrium and rare-earth elements in the Penge
404 and Kuruman iron-formations, Transvaal Supergroup, South Africa. *Precambrian*
405 *Research* **79,** 37–55 (1996).

52. Sunda, W. G. & Huntsman, S. A. Effect of sunlight on redox cycles of manganese in the southwestern Sargasso Sea. *Deep Sea Research Part A. Oceanographic Research Papers* **35,** 1297–1317 (1988).
53. Bau, M., Koschinsky, A., Dulski, P. & Hein, J. R. Comparison of the partitioning behaviours of yttrium, rare earth elements, and titanium between hydrogenetic marine ferromanganese crusts and seawater. *Geochimica et Cosmochimica Acta* **60,** 1709–1725 (1996).
54. Byrne, R. H., Liu, X. & Schijf, J. The influence of phosphate coprecipitation on rare earth distributions in natural waters. *Geochimica et Cosmochimica Acta* **60,** 3341–3346 (1996).
55. German, C. R. & Elderfield, H. Application of the Ce anomaly as a paleoredox indicator: The ground rules. *Paleoceanography* **5,** 823-833 (1990).
56. Shields, G. & Webb, G. Has the REE Composition of Seawater Changed Over Geological Time? **204.1**, 103–107 (2004).
57. Poulton, S. W. & Canfield, D. E. Development of a sequential extraction procedure for iron: implications for iron partitioning in continentally derived particulates. *Chemical Geology* **214,** 209–221 (2005)
58. Canfield, D. E., Raiswell, R., Westrich, J. T., Reaves, C. M. & Berner, R. A. The use of chromium reduction in the analysis of reduced inorganic sulfur in sediments and shales. *Chemical Geology* **54,** 149–155 (1986).

Acknowledgements

RT, RAW, GASZ, SWP, RG, FB, ARP acknowledge financial support from NERC's Co-evolution of Life and the Planet scheme (NE/1005978/1). Support was provided to MOC and ARP through the International Centre for Carbonate Reservoirs (ICCR). FB acknowledges support from the Laidlaw Hall fund. We are grateful for access to farms, and thank A. Horn of Omkyk, U. Schulze Neuhoff of Ababis, L. and G. Fourie of Zebra River, C. Husselman of Driedornvlagte, and L. G. Evereet of Arasab and Swartpunt. We thank Gary Tarbuck and Jim Davy for technical support, and Gerd Winterleitner and Tony Prave for help carrying out field work.

Author contributions

RAW, ARP, KHH, RT, AMP, FB, and AC collected the samples. MOC, RT, AMP and FB prepared the samples. RT conceived the project and analysed the samples. RT interpreted the Ce anomaly data, after discussions with GAS, TH, RG and SWP. RT wrote the paper, with significant input from GAS, SWP, RAW, and RG.

Figure 1

Schematic representation of redox zones and associated geochemical signals in the Zaris Basin, Nama Group during a highstand systems tract. Positive Ce anomalies form as Mn (oxyhydr)oxides dissolve in the manganous zone, and Fe enrichments form under anoxic ferruginous conditions. 10 μM is an estimate of maximum O_2 concentrations in the manganous zone, but overlying well-oxygenated waters may have contained higher O_2 concentrations. Representative REY patterns, including positive Ce anomalies (magnitude in brackets), are shown for the Omkyk section in

the Nama Group, alongside manganous zones from two modern environments[20,22] (modern water column data plotted as [REY] × 10^6 to be comparable with sedimentary [REY]).

Figure

The location of nine sections within the Kuibis and Schwarzrand Subgroups of the Nama Group is shown on a simplified geological map of Namibia (top left), as well as on a schematic cross section indicating average relative water depth (bottom). Fe_T data for each location is shown for carbonate and siliciclastic rocks, colour coded for redox interpretation based on Fe_{HR}/Fe_T and Fe_T[5], alongside Ce_{SN}/Ce^*_{SN} data, screened for carbonate rocks showing seawater REY patterns (e.g. molar Y/Ho>67). Blue Fe_T data indicate where Fe speciation would predict oxic conditions[5], and positive Ce anomalies indicate where oxic waters are interpreted to have been manganous. The presence of *in situ* biota is noted by grey lines[5].

Figure

Mn/Fe ratios for samples identified as manganous (positive Ce/Ce* and low Fe_T or oxic Fe-speciation signals), ferruginous (anoxic Fe-speciation signals) and oxic (oxic Fe-speciation signals, no positive Ce anomaly). Mn/Fe is enriched in manganous samples compared with global carbonate (0.29)[Ref 49]. Bars represent median values. Red outlines indicate dolomitised samples.

Figure 4

A comprehensive redox interpretation is shown for each of the nine localities in the Nama Group, determined using combined Fe and Ce signals (see inset table). *In situ* fossils (grey lines), and local ecologies[5] and general ecology from the literature[30,31] are shown alongside local water column redox conditions. The bar chart plots the frequency that different biota are found in each redox zone[5]. Large skeletal fossils and burrows are found exclusively in well-oxygenated settings, and small skeletal fossils are largely restricted to well-oxygenated conditions, but may occur where conditions were only fleetingly oxic.

Figure 1

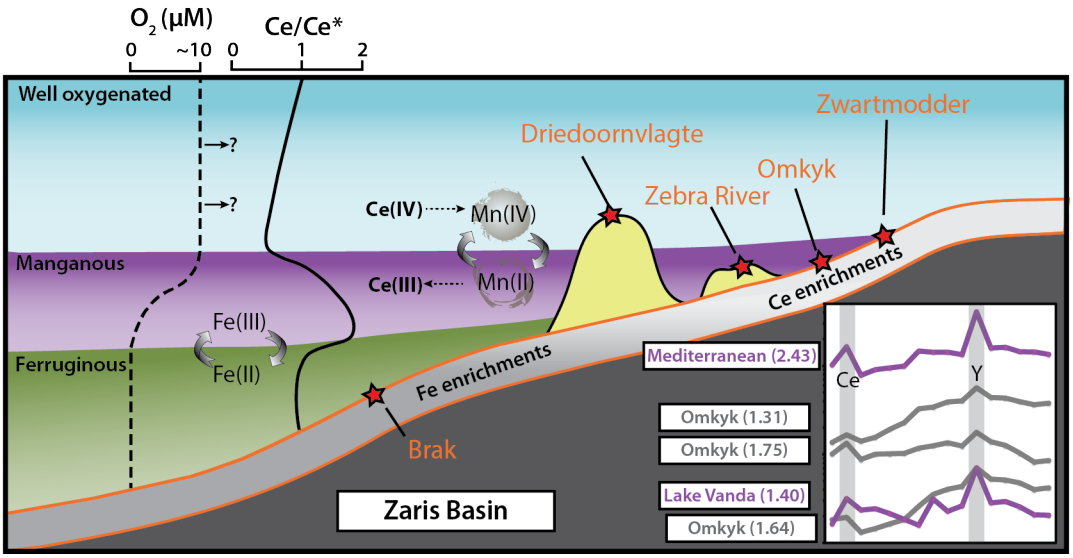

Figure 2

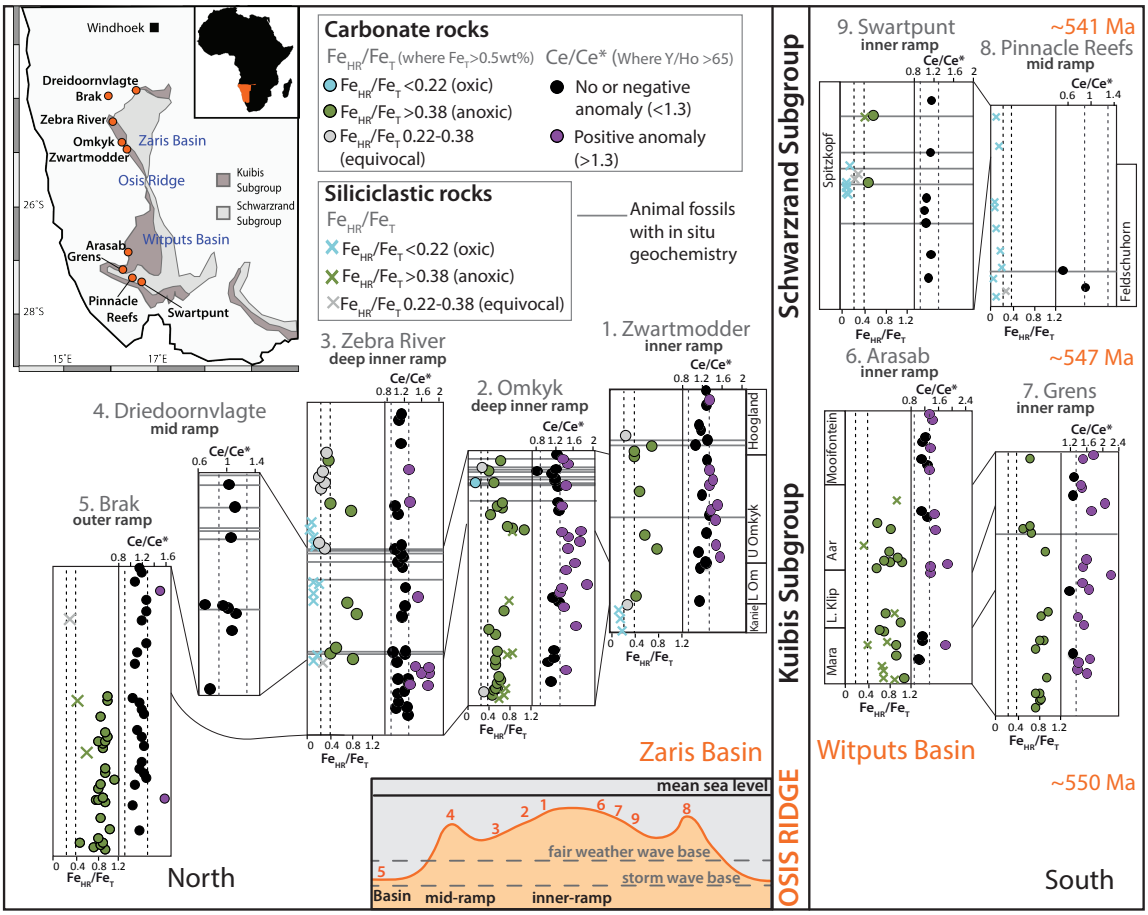

489

490 **Figure 3**

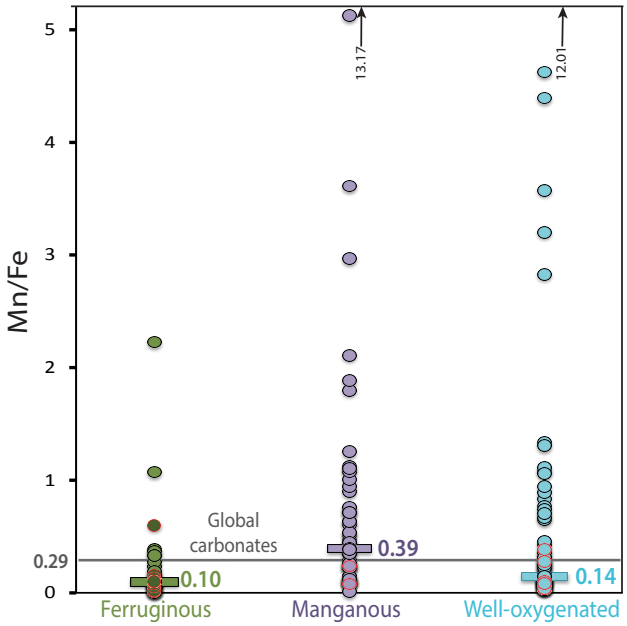

491

492 **Figure 4**

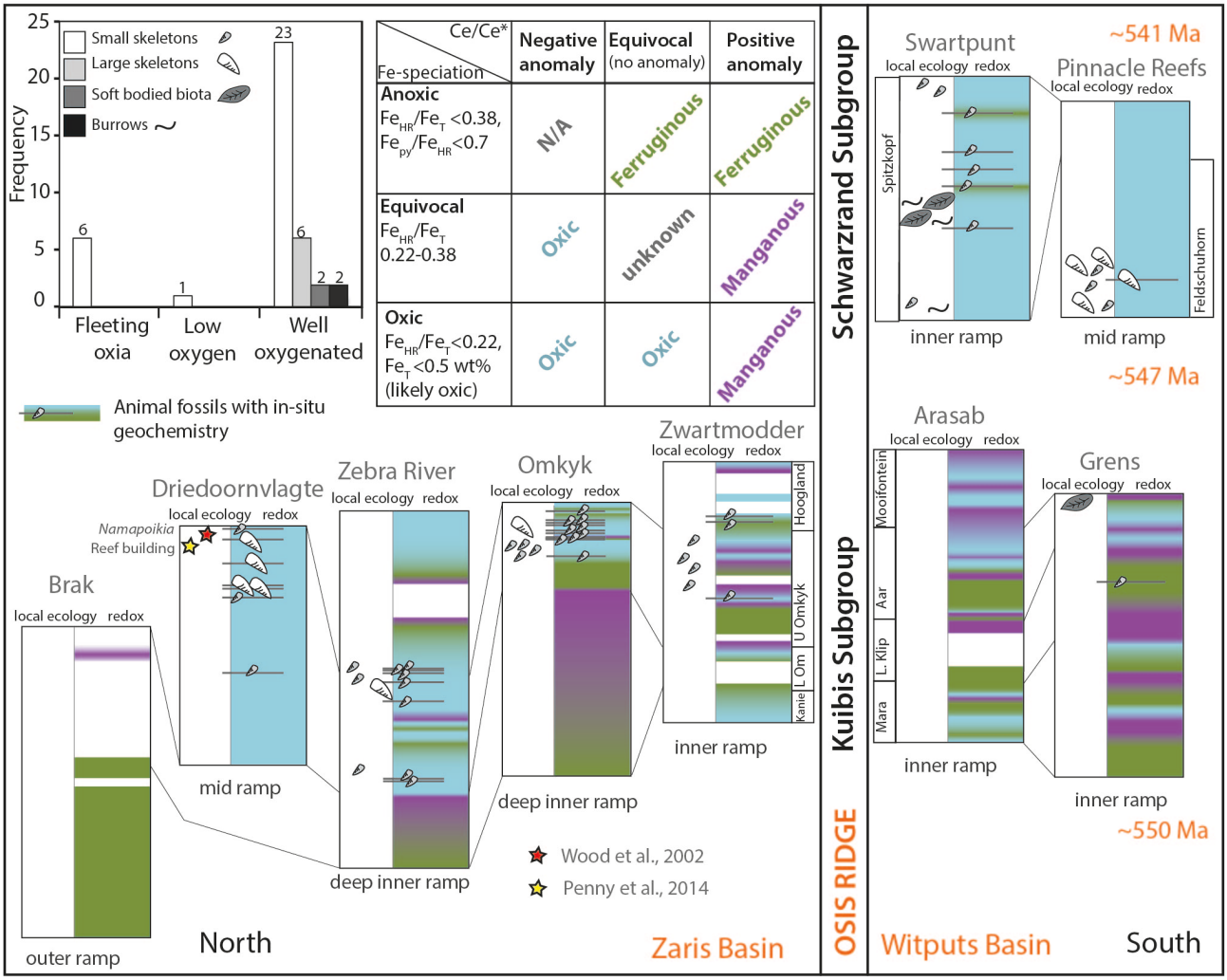

493
494
495

Methods

Samples from nine shelf-to-basin sections within the Zaris and Witputs basins of the Nama Group encompass a range of palaeo-depths from outer- to inner-ramp settings. Stratigraphic correlations are well-established based on sequence boundaries and ash beds[5,29]. Unweathered samples were selected, and powdered or drilled avoiding alteration, veins or weathered edges. For Zebra River section, powders were drilled from thin section counterparts, targeting fine grained cements. Carbonate rocks in the Nama Group are very pure, but they have all undergone pervasive recrystallisation. Less than 15% of the samples in this study are dolomitised, and there is no petrographic evidence for deep burial dolomitisation in the Nama Group[5,50] Most carbonate rocks are associated with low Mn/Sr ratios and heavy $\delta^{18}O$ (see Supplement information). The presence of different forms of skeletal biota, soft-bodied biota, trace fossils are reported for precise horizons where geochemical analyses have been performed[5], indicated by grey lines on Figs 2 and 3. General local ecology, supported by additional information from the literature, is also marked, without associated grey lines. Our sampling focused on carbonates, and hence skeletal fossils are over-represented compared with soft-bodied biota and trace fossils. We define 'large' skeletal animals as >10 mm in any dimension, which includes *Cloudina hartmannae,* some *Namacalathus,* and *Namapoikia*.

Rare earth elements

Rare earth elements and yttrium (REY) have a predictable distribution pattern in seawater, and non-biological carbonate rocks should preserve local water column REY at the sediment-water interface[23]. Ce anomalies develop progressively, but cut-off values are established to define negative and positive anomalies. We define a negative anomaly as Ce_{SN}/Ce^*_{SN} <0.9, consistent with previous work[51]. A positive anomaly, using the same reference frame, would be defined as Ce_{SN}/Ce^*_{SN} >1.1. But since positive anomalies are not previously described from carbonate sediments, we cautiously use a higher cut off, Ce_{SN}/Ce^*_{SN} >1.3, to ensure any positive anomalies are environmentally significant with respect to positive anomalies recorded from some modern manganous waters (1.21-2.43) (see supplementary information for discussion of Ce_{SN}/Ce^*_{SN} cut-offs). While positive or negative Ce anomalies in carbonate rocks likely represent seawater redox conditions, the absence of any Ce anomaly (0.9-1.3) is somewhat equivocal, and could result from anoxic water column conditions, or overprinting of any Ce anomaly during diagenesis or leaching[26]. Alternately, Ce anomaly formation may be disrupted in surface waters because of wind-blown dust or photo-reduction of Mn oxides[52]. Fe (oxyhydr)oxides may also be REY carriers, but do not contain the clear Ce enrichments observed in Mn (oxyhydr)oxides (see Supplementary Information for full discussion of REY carriers).

Diagenetic phosphates, Fe and Mn (oxyhydr)oxides, organic matter and clays can potentially affect the REY signatures of authigenic sedimentary rocks if they are partially dissolved during the leaching process[53–56]. Care has been taken to partially

leach samples, to isolate the carbonate phase without leaving excess acid, which may leach contaminant phases (see Ref 26 for detailed discussion of methodology). Powdered calcite samples were cleaned in Milli–Q water and pre–leached in 2% nitric acid to remove adsorbed and easily exchangeable ions associated with clay minerals. The remaining sample was partially leached, also in 2% (w/v) nitric acid, to avoid contributions from contaminant phases such as oxides and clays[26]. The supernatant was removed from contact with the remaining residue, diluted with 2% nitric acid and analysed via inductively coupled plasma mass spectrometry in the Cross–Faculty Elemental Analysis Facility, University College London. This leaching method has been designed to extract the carbonate bound REY pool without contributions from (oxyhydr)oxides or clays[26]. These same leachates were also analysed for major element concentrations (Mg, Fe, Mn, Al and Sr) via inductively coupled plasma optical emission spectrometry. Oxide interference was monitored using the formation rate of Ce oxide, and the formation of 2+ ions was monitored using Ba^{2+}. All REY concentrations were normalised to post-Archean Australian Shale (PAAS). Ce anomalies were calculated using equation (1).

Standard solutions analysed after every ten samples were within 5% of known concentrations. Replicate analyses on the ICP-MS give a relative standard deviation <5% for most trace elements, with a larger standard deviation for the heavy REE that sometimes have non-normalised concentrations <0.5 ppb. Carbonate standard material CRM 1c was prepared using the same leaching procedure as the samples, and repeat analyses give a relative standard deviation <5% for individual REY

564 concentrations, and calculated Ce anomalies (average=0.80) give a relative standard
565 deviation <3%.
566
567 Mn/Sr ratios are <1 for the majority (97%) of samples, and δ^{18}Ocarb is >-10‰,
568 indicating minimal open-system elemental and isotopic exchange during diagenesis,
569 and excluding deep burial dolomitisation (Fig S3). Ce anomaly data are only
570 presented for carbonates that preserve seawater REY features (smooth patterns
571 with molar Y/Ho>67)[23,26] indicating they originate from the carbonate portion of the
572 whole rock, without contributions from detrital or oxide phases. For samples with
573 Y/Ho>67, 85% also have ∑REE <2 ppm, and all have ∑REE <10 ppm. La anomalies,
574 and small positive Eu and Gd enrichments, are prevalent in samples with Y/Ho>67.
575 Positive Ce anomalies are associated with low Mn/Sr ratios (<1) and low Al, Zr, Ti,
576 Fe and Mn contents in the leachate (<0.2 wt% for Fe, and <500 ppm for Mn),
577 indicating minimal contamination due to diagenetic exchange, leaching of clays or
578 Fe-Mn (oxyhydr)oxide phases (see Supplementary Information for a full assessment
579 of data quality).
580
581 **Fe speciation**
582 The Fe speciation method quantifies Fe that is (bio)geochemically available in
583 surficial environments (termed highly reactive Fe; Fe_{HR}) relative to total Fe (Fe_T).
584 Mobilisation and subsequent precipitation of Fe in anoxic water column settings
585 results in Fe_{HR} enrichments in the underlying sediment. The nature of anoxia (i.e.
586 sulphide-rich or Fe-containing) is determined by the extent of sulphidation of the

highly reactive Fe pool[1]. Fe speciation data for carbonate rock samples discussed here, and accompanying interbedded siliciclastic rocks, come from previously published data[5]. The Fe-speciation technique was performed using well established sequential extraction schemes[29]. The method targets operationally defined Fe pools, including carbonate-associated-Fe (Fe_{Carb}), ferric oxides (Fe_{Ox}), magnetite (Fe_{Mag}), pyrite Fe (Fe_{Py}) and Fe_T. Fe_{HR} is defined as the sum of Fe_{carb} (extracted with Na-acetate at pH 4.5 and 50˚C for 48h), Fe_{ox} (extracted via Na-dithionite at pH 4.8 for 2h), Fe_{mag} (extracted with ammonium oxalate for 6h) and Fe_{py} (calculated from the mass of sulphide extracted during $CrCl_2$ distillation). Fe_T extractions were performed on ashed samples (8 h at 550˚C) using HNO_3–HF–H_3BO_3–$HClO_4$. All Fe concentrations were measured via atomic absorption spectrometry and replicate extractions gave a relative standard deviation of <4% for all steps, leading to <8% for calculated Fe_{HR} (see Supplementary Information for full discussion of data quality). Fe_{Py} was calculated from the wt% of sulphide extracted as Ag_2S using hot Cr(II)Cl_2 distillation[58]. A boiling HCl distillation before the Cr(II)Cl_2 distillation ruled out the potential presence of acid volatile sulfides in our samples. Pyrite extractions give reproducibility for Fe_{py} of 0.005 wt%, confirming high precision for this method. Analysis of a certified reference material (PACS-2, Fe_T = 4.09 ± 0.07 wt%, *n* = 4; certified value = 4.09 ± 0.06 wt%) confirms that our method is accurate. Replicate analyses (*n* = 6) gave a precision of ± 0.06 wt% for Fe_T, and a relative standard deviation of <5% for the Fe_{HR}/Fe_T ratio.

609 Calibration in modern and ancient marine environments suggests that Fe_{HR}/Fe_T
610 <0.22 indicates deposition under oxic water column conditions, while Fe_{HR}/Fe_T
611 >0.38 indicates anoxic conditions[1]. Ratios between 0.22–0.38 are considered
612 equivocal, and may represent either oxic or anoxic depositional conditions. For
613 sediments identified as anoxic, Fe_{py}/Fe_{HR} >0.8 is diagnostic for euxinic conditions
614 and Fe_{py}/Fe_{HR} <0.7 defines ferruginous deposition[1]. This also applies to carbonate-
615 rich sediments that have not undergone late stage dolomitisation[28], on the condition
616 that Fe_T >0.5wt%. Where Fe_T is very low (<0.5wt%), this may indicate deposition
617 under oxic conditions[28]. However, wherever possible we consider together data
618 obtained from siliciclastic horizons interbedded with and/or associated with
619 carbonate rocks contained within the same m- to dm-scale depositional cycle. Fe-
620 speciation in carbonate and siliciclastic rocks gives consistent signals in the Nama
621 Group (Figure 2), supporting the application of this proxy in carbonate rocks[5,28]